WILEY-VCH

Udo J. Birk

# Super-Resolution Microscopy

## A Practical Guide

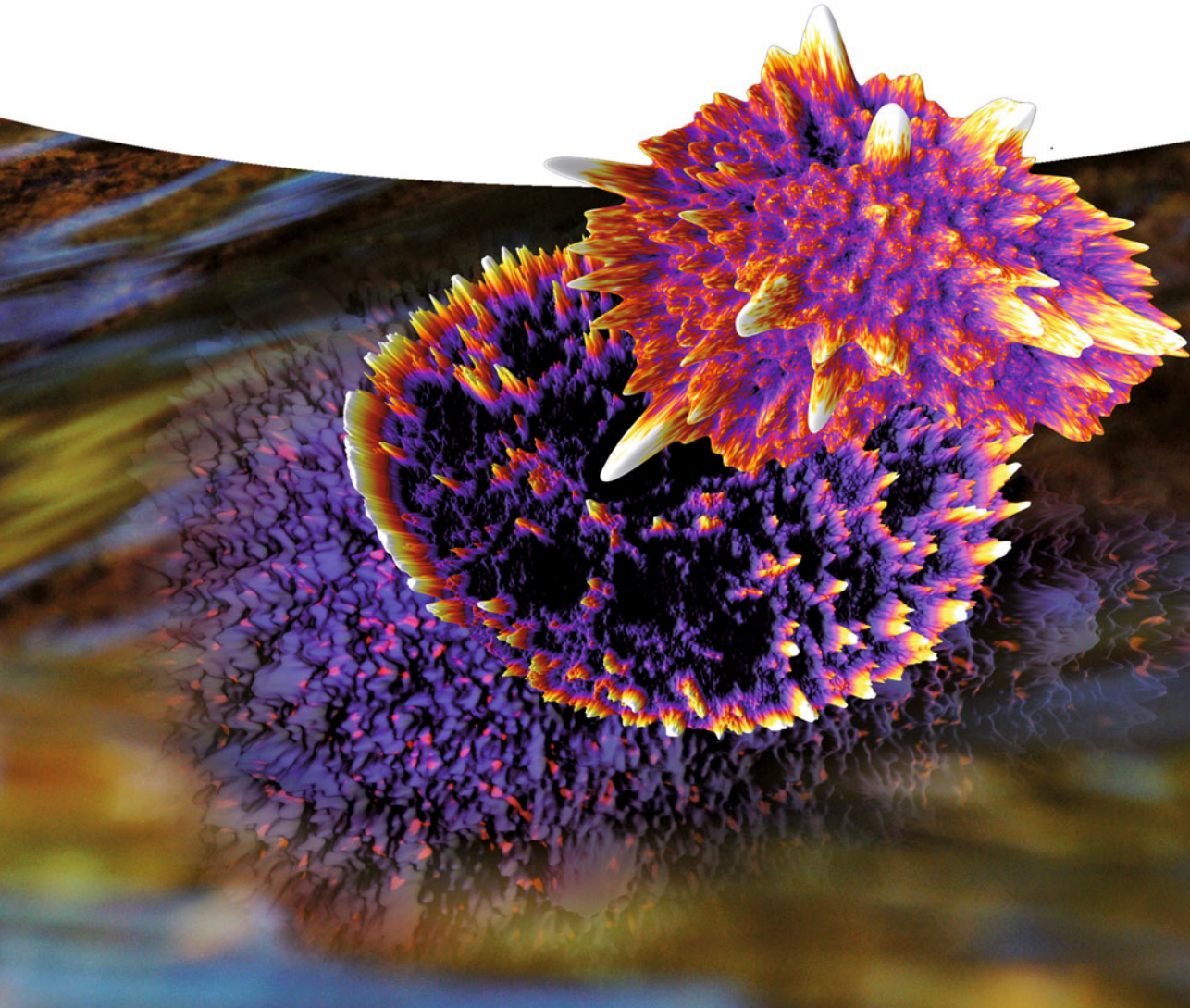

*Udo J. Birk*

# Super-Resolution Microscopy

*Udo J. Birk*

# Super-Resolution Microscopy

A Practical Guide

WILEY-VCH
Verlag GmbH & Co. KGaA

**Author**

***Udo J. Birk***
Institute of Molecular Biology (IMB) GmbH
Ackermannweg 4
55128 Mainz
Germany

and

Johannes Gutenberg University Mainz
Institute of Physics
Staudinger Weg 7
55128 Mainz
Germany



**Library of Congress Card No.:**
applied for

**British Library Cataloguing-in-Publication Data:**
A catalogue record for this book is available from the British Library.

**Bibliographic information published by the Deutsche Nationalbibliothek**
The Deutsche Nationalbibliothek lists this publication in the Deutsche Nationalbibliografie; detailed bibliographic data are available on the Internet at http://dnb.d-nb.de.



**Cover Design** Adam-Design, Weinheim, Germany
**Typesetting** le-tex publishing services GmbH, Leipzig, Germany

**Print ISBN** 978-3-527-34133-7
**ePDF ISBN** 978-3-527-80206-7
**ePub ISBN** 978-3-527-80208-1
**Mobi ISBN** 978-3-527-80205-0
**oBook ISBN** 978-3-527-80207-4

Printed on acid-free paper.

This book is for Hanne and Maris
and for Li.

## Contents

**Preface** *XIII*

**Abbreviations** *XV*

**1 Introduction** *1*
1.1 Classical Resolution Limit *3*
1.1.1 Examples of Microscopic Imaging without Using Visible Light *7*
1.1.2 Early Concepts of Enhanced Optical Resolution *9*
1.1.3 Two-Photon and Near-Field Optical Microscopy *12*
1.2 Methods to Circumvent the Classical Resolution Barrier in Fluorescence Microscopy *13*
1.2.1 Interferometric Microscopy *14*
1.3 Implementation of Super-Resolution Microscopy *16*
1.4 Contrast *24*
1.4.1 Multi-Color Imaging *26*
1.5 Applications to the Study of Nuclear DNA *27*
1.6 Other Applications *30*
References *30*

**2 Physicochemical Background** *41*
2.1 Motivation *41*
2.2 Labeling *42*
2.2.1 Fluorophores *42*
2.2.2 Methods of Labeling *52*
2.2.3 Labeling Density *57*
2.2.4 Binding *58*
2.3 Fluorophore Transitions *59*
2.3.1 Photobleaching *61*
2.3.2 Photoswitching and Photon Yield *63*
2.3.3 How to Achieve Switching, Blinking, Photostability, and High Photon Yield *66*
2.3.4 Buffer Solutions for Combinations of Fluorophores *71*
2.4 Samples *71*

2.4.1 Optical Properties *71*
2.4.2 Effects of Motion *74*
2.4.3 Fixation *74*
2.4.4 Diffusion *75*
2.4.5 *In vivo* *75*
References *76*

**3 Hardware and Software** *83*
3.1 Hardware Requirements *83*
3.1.1 Collection of Fluorescence *84*
3.1.2 Detectors *86*
3.1.3 llumination *90*
3.1.4 Adaptive Optics *92*
3.1.5 Computer Technology *94*
3.1.6 Overall System *96*
3.2 Software *97*
3.2.1 Feature Extraction *98*
3.2.2 Error Correction *102*
3.2.3 Visualization *107*
3.2.4 Meta-Analysis *108*
3.2.5 Confidence Analysis *109*
3.3 Open Source and Best Practice *110*
References *111*

**4 Structured Illumination and Image Scanning Microscopy** *117*
4.1 Axially Structured Illumination Microscopy *118*
4.1.1 aSIM Setup *119*
4.1.2 Principles of aSIM Size and Position Measurement *123*
4.1.3 Requirements and Sample Preparation *125*
4.1.4 Data Acquisition *127*
4.1.5 Data Analysis and Visualization *129*
4.1.6 Example Applications *132*
4.2 Laterally Structured Illumination Microscopy *134*
4.2.1 Principles of Lateral SIM *136*
4.2.2 Implementation of Lateral SIM *138*
4.2.3 Requirements and Sample Preparation *142*
4.2.4 Data Acquisition *146*
4.2.5 Data Analysis and Visualization *147*
4.2.6 Example Applications *150*
4.2.7 Imaging DNA Repair *156*
4.3 Image Scanning Microscopy *157*
4.3.1 Principles of Image Scanning Microscopy *158*
4.3.2 Implementation of Image Scanning Microscopy *159*
4.3.3 Requirements and Sample Preparation *161*
4.3.4 Data Analysis and Visualization *162*

4.3.5 Example Applications *164*
4.3.6 Conclusion *164*
4.4 Super-Resolution Using Rotating Coherent Scattering (ROCS) Microscopy *166*
4.4.1 Principles of ROCS *166*
4.4.2 ROCS Image Generation *168*
4.4.3 Conclusion *170*
References *171*

**5 Localization Microscopy** *179*
5.1 Principles of Localization Microscopy *179*
5.2 PALM/STORM/fPALM/SPDM Approach *181*
5.3 Implementation of SMLM *185*
5.4 Principles of Three-Dimensional SMLM *187*
5.5 Reduction of Out-of-Focus Light *188*
5.6 How to Build a Three-Dimensional SMLM *189*
5.7 High-Density Single-Emitter Microscopy Methods: SOFI, 3B, SHRImP, and Others *196*
5.7.1 Independent Component Analysis *196*
5.7.2 Single-Molecule High-Resolution Imaging with Photobleaching *197*
5.7.3 Super-Resolution Optical Fluctuation Imaging (SOFI) *199*
5.7.4 Bayesian Analysis of Blinking and Bleaching *200*
5.7.5 Binding- and Activation-Assisted Separation *202*
5.8 Approaches to Counting Molecules *202*
5.8.1 Stepwise Photobleaching *203*
5.8.2 Intensity Histogram Analysis *203*
5.8.3 Multi-Color Colocalization *205*
5.9 Requirements and Sample Preparation *206*
5.9.1 Microtubule Staining for $SPDM_{phymod}$ and dSTORM *207*
5.9.2 Imaging Buffer *208*
5.9.3 Sampling *209*
5.9.4 Counterstaining *209*
5.9.5 Selection of Fluorophores *210*
5.9.6 Cross-Talk *210*
5.9.7 Illumination *213*
5.10 Data Acquisition *214*
5.11 Data Analysis *218*
5.11.1 Effect of Threshold and Signal Detection *219*
5.11.2 Extraction of Position, Photon Count, and Other Parameters *220*
5.11.3 Excluding Imprecise Localizations *222*
5.11.4 Assessing Image Resolution in SMLM *223*
5.11.5 Available Software for SMLM Data Analysis *223*
5.12 Troubleshooting *225*
5.13 Meta Analysis Tailored for SMLM *227*

5.13.1 Structure Averaging in Localization Microscopy *228*
5.13.2 Pair Correlation Analysis *228*
5.13.3 Analyzing Single-Molecule Trajectories *237*
5.14 Example Applications *245*
5.14.1 Multi-Color SMLM *245*
5.14.2 Live-Cell SMLM *246*
5.14.3 Structural Biology *247*
5.14.4 Imaging in the Neurosciences *248*
5.14.5 SMLM Spectroscopy *248*
5.14.6 Example Applications to Chromatin Nanostructure *249*
5.14.7 Combining Multiple Imaging Approaches *250*
References *252*

**6 Stimulated Emission Depletion Microscopy** *263*
6.1 Principles of Stimulated Emission Depletion Microscopy *266*
6.2 Implementation of STED *270*
6.2.1 Pulsed STED (p-STED) *270*
6.2.2 Continuous Wave STED *271*
6.2.3 Gated cw STED *272*
6.2.4 Protected STED *274*
6.2.5 Generation of the STED Beam PSF *275*
6.3 Fluorescent Probes *277*
6.4 Dye Combinations for Dual-Color STED *279*
6.5 Requirements and Sample Preparation *282*
6.5.1 Base Instrument *282*
6.5.2 Laser Light Sources *282*
6.5.3 Choice of Detector *285*
6.5.4 Obtaining a High-Quality PSF *289*
6.5.5 Embedding Media *290*
6.5.6 Sample Preparation Protocol *292*
6.6 Data Acquisition *293*
6.6.1 Adjusting for Cover Glass Thickness Using Correction Collar Ring *293*
6.6.2 Pixel Size, Scan Speed, and Averaging *294*
6.6.3 Adjust the Laser Power of the STED Depletion Beam *295*
6.6.4 Increase the Signal from a STED Sample *295*
6.7 Data Analysis and Visualization *297*
6.7.1 Spectral Unmixing *297*
6.7.2 Deconvolution *298*
6.8 Example Applications *298*
6.8.1 Multi-Color STED *298*
6.8.2 Ultra-High-Resolution STED *299*
6.8.3 *In-Vivo* STED *299*
6.8.4 Deep Tissue Imaging *301*
6.8.5 Imaging Fast Dynamics *303*

6.8.6 Imaging Nuclear Chromatin *305*
6.8.7 Imaging Techniques Combined with STED *307*
6.9 Conclusion *309*
References *310*

**7 Multi-Scale Imaging** *315*
7.1 Light-Sheet Fluorescence Microscopy *316*
7.1.1 Principle of LSFM *317*
7.1.2 Data Analysis and Visualization *321*
7.1.3 Sample Preparation and Sample Mounting *323*
7.1.4 Example Applications *324*
7.1.5 Conclusion *328*
7.2 Optical Projection Tomography *329*
7.2.1 Principles of 3D Image Formation in OPT *330*
7.2.2 OPT Setup *332*
7.2.3 Requirements and Sample Preparations *333*
7.2.4 Data Acquisition and Reconstruction *334*
7.2.5 Example Applications *336*
7.2.6 Conclusion *338*
7.3 Expansion Microscopy and Sample Clearing *339*
7.3.1 Principles of Expansion Microscopy *339*
7.3.2 Implementation of Expansion Microscopy *340*
7.3.3 Example Applications *342*
7.3.4 Clearing *343*
7.3.5 Conclusion *348*
7.4 Alternative Approaches *348*
References *349*

**8 Discussion** *357*
8.1 Future Challenges *357*
8.1.1 Super-Resolution Microscopy Structural Analysis in Linear Excitation Mode *358*
8.1.2 Quantification *360*
8.1.3 *In-Vivo* Experiments Using STED and SMLM *361*
8.1.4 Enhancement of Resolution *362*
8.1.5 Multi-Color Experiments *363*
8.1.6 Photophysics and the Development of Reporter Molecules *366*
8.1.7 Novel Labeling Strategies *367*
8.1.8 Fast and Accurate Software *368*
8.1.9 Next-Generation Computing Hardware *368*
8.1.10 Imaging of 3D Extended Objects *369*
8.1.11 Super-Resolution Microscopy with a Large Field of View *369*
8.1.12 Multi-Modal, Correlative Super-Resolution Imaging *370*
8.1.13 Super-Resolution in Routine Applications *371*
8.1.14 Super-Resolution Using Other Contrast Mechanisms *372*

8.2 Commercialization of Super-Resolution Microscopes *372*
8.3 Concluding Remarks *373*
References *374*

**Index** *379*

# Preface

'Many hands make light work.'

… and both meanings of the proverb sound true to me: The success of super-resolution microscopy based on laser light doing what it is supposed to do is the result of the hard work of many researchers worldwide. And for many of us members of the global scientific communities, trying to find answers to questions such as "why?" and "what for?" is an integral part of our everyday lives. Naturally I had to wrestle with these issues during the writing process of this book as well, although it seems to me that the reasons for the endeavor and its potential functions might coalesce in this case.

Rendering entities or structures visible that could not be seen before, while reflecting on – and calling into doubt – the visualization strategies employed is an as beautiful and valuable process as it is a tricksterish one. Furthermore, it is fair to say that particularly the rather young research area of super-resolution microscopy has proven to be tremendously productive for applications ranging from molecular and structural biology to developmental biology to neuroscience. Advancements in the field of biomedicine are an especially clear paradigmatic example of the social relevance of applied photonics in this multi-disciplinary research field because it is a fact that progress in, for example, early cancer diagnosis or drug development strategies may contribute to healthier and longer lives for all of us.

This book, in addition to being a tribute to the hard work of super-resolution specialists around the world, was written to be a key educational resource, a handbook, i.e., according to genre conventions, specifically designed for the dissemination of knowledge and skills. This reflects the fact that the main parts of the book originated in a lecture series on biomedical optics given at the universities of Heidelberg and Mainz in 2013–2016. Hopefully the publication will prove to be a useful means of support in learning processes for senior researchers – who are curious to understand ever more – as much as for coming generations of scientists.

But there is another correlation between learning processes and the book that you hold in your hands; it simply would not be there without the teachers I myself

have had the privilege of being educated by. I want to express my sincerest gratitude to Prof. Dr. Christoph Cremer, one of the most eminent scholars in the field. I cannot put into words what I have learned from him in the last years: Ich danke Ihnen von ganzem Herzen. Many heartfelt thanks to Prof. Dr. Jorge Ripoll Lorenzo for his incredible help and support, for his friendship and trust; ευχαριστώ πάρα πολύ, from you I have learned so much, especially how powerful ideas can really be. Special thanks go to Prof. Dr. Rainer Heintzmann, not only for the fantastic welcome he gave me at King's College London during my time as a Marie Curie Fellow on his research team but for his always helping hand as well as helping mind and for our productive collaborations. I am also deeply grateful for all the expertise, wonderful support, and great help provided to me by Prof. Dr. Vasilis Ntziachristos. Thank you so much, Prof. Dr. Gerd Schönhense, for your excellent counsel, for your encouragement, and for being my mentor during the habilitation process at the Johannes Gutenberg University in Mainz, Germany. And I would like to extend my sincere gratitude to the (to me unknown) referees of my habilitation for their support. I am also deeply indebted to Prof. Dr. Michael Hausmann for his encouragement, wonderful help and guidance over the years. I would like to express my deep gratitude to Dr. Waltraud Wüst and Dr. Marcel Reuter from Wiley-VCH for their expertise and for making the book see the light of day. And needless to say, this book could never have been written without the support and encouragement from my colleagues, especially at the Core Facility Microscopy, and the members of Prof. Cremer's teams at the Institute of Molecular Biology (IMB) Mainz and the Institute of Pharmacy and Molecular Biotechnology (IPMB) Heidelberg. Love to my families in Freiburg, Offenburg, Endingen and Engen. Many thanks to you all.

"[O]nce a story is told, it cannot be called back. Once told, it is loose in the world" [1]. This story of super-resolution microscopy is being set free in the hope that it may do its job of providing an ever so small contribution to the generation of new ideas in a self-reflexive and responsible manner, to the sharing of ideas in a transcultural scientific community, and to finding applications that might one day serve humanity or keep our environment healthy and alive.

Mainz, Germany, April 2017 *Udo Birk*

**Reference**

1 King, T. (2008) *The Truth About Stories: A Native Narrative*, Univ. of Minnesota Press, Minneapolis, 1st edn.

## Abbreviations

| | |
|---|---|
| 2P | two-photon excitation |
| 2D, 3D | two-dimensional, three-dimensional |
| 3B | Bayesian analysis of blinking and bleaching |
| ADU | analog-to-digital unit (digitization of detector signals) |
| AID | axial intensity distribution |
| aSIM | axially structured illumination microscopy |
| BABB | 1 : 2 benzyl alcohol : benzyl benzoate |
| BMMs | biomolecular machines |
| bp | basepairs, number of bases in nucleic acids |
| BrdU | 5-bromo-2′-deoxyuridine |
| BSA | bovine serum albumin |
| CCD | charge-coupled device (camera) |
| CLSM | confocal laser scanning microscope |
| CMOS | complementary metal-oxide semiconductor (camera) |
| CNR | contrast-to-noise ratio |
| COI | center of intensity |
| CRISPR | clustered regularly interspaced short palindromic repeat |
| Cy3, Cy5 | fluorophores: cyanine dyes |
| DABCO | 1,4-diazabicyclo[2.2.2]octan |
| DNA | deoxyribonucleic acid |
| DOF | depth of field, depth of focus |
| EdU | 5-ethynyl-2′-deoxyuridine |
| EM | electron microscopy |
| EMCCD | electron-multiplying charge-coupled device (camera) |
| ExM | expansion microscopy |
| FDR | frequency-distance relation (in tomography) |
| FISH | fluorescence *in situ* hybridization |
| FOV | field of view |
| fPALM | fluorescence photoactivation localization microscopy |
| fps | frames per second |
| FRET | fluorescence (Förster) resonance energy transfer |
| FWHM | full width at half-maximum |

| | |
|---|---|
| GFP | green fluorescent protein |
| GLOX | glucose oxidase-based oxygen-scavenging buffer |
| GPU | graphics processing unit |
| GSD | ground state depletion |
| HaloTag | modified enzyme that can be fused to any protein of interest for further detection (e.g., via fluorescence labeling) |
| HILO | highly inclined and laminated thin optical light sheet |
| HPD | hybrid photodetector |
| iPALM | interferometric photoactivated localization microscopy (a special type of 3D localization microscopy) |
| IR | infrared |
| ISC | intersystem crossing (electronic transition) |
| kDa | kilodalton, 1000 unified atomic mass units |
| LED | light-emitting diode |
| LSFM | light sheet fluorescence microscopy |
| LSE | least squares estimation |
| LSI | linear shift invariant |
| MEA | β-mercaptoethylamine, also known as cysteamine |
| MLE | maximum likelihood estimation |
| MSIM | multi-focal structured illumination microscopy |
| NA | numerical aperture |
| NGS | next-generation sequencing |
| OPT | optical projection tomography |
| OTF | optical transfer function |
| PALM | photoactivated localization microscopy |
| PALMIRA | PALM with independently running acquisition |
| PBS | phosphate buffered saline |
| PDF | probability density function |
| PEM | patterned excitation microscopy |
| pixel | picture element |
| PMT | photomultiplier tube |
| Pol II | polymerase II |
| PSF | point spread function |
| RNA | ribonucleic acid |
| ROI | region of interest |
| ROCS | rotating coherent scattering |
| ROXS | reducing and oxidizing buffer system |
| sCMOS | scientific complementary metal-oxide semiconductor (camera) |
| SIM | structured illumination microscopy |
| SMLM | single-molecule localization microscopy |
| SNR | signal-to-noise ratio |
| SNAP-tag | polypeptide that can be fused to any protein of interest for further detection (e.g., via fluorescence labeling) |
| SOFI | super-resolution optical fluctuation imaging |
| SPAD | single-photon-counting silicon avalanche photodiode |

| | |
|---|---|
| SPDM | spectral precision distance microscopy/spectral position determination microscopy |
| SPEM | saturated patterned excitation microscopy |
| SPIM | selective or single-plane illumination microscopy |
| SSIM | saturated structured illumination microscopy |
| STD | standard deviation |
| STED | stimulated emission depletion |
| STORM | stochastic optical reconstruction microscopy |
| TAD | topologically associating domain |
| TALE-N | artificial nuclease based on transcription activator-like effectors |
| TDE | 2,2′-thiodiethanol |
| TIR | total internal reflection |
| VIM | virtual microscopy |
| voxel | volume element in 3D digital images |
| WLC | worm-like chain (model in polymer physics) |
| xFP | any fluorescent protein, for example, GFP or YFP |
| YFP | yellow fluorescent protein |

# 1
# Introduction

"To see a World in a Grain of Sand" (William Blake) [1] – "not only one world and not only in a grain of sand," a researcher working in the field of super-resolution microscopy might comment. Advanced far-field light-optical methods have become an indispensable tool in the analysis of nanostructures with applications both in the field of material sciences and in the life sciences. Tremendous progress has been made in recent years in the development and application of novel super-resolution fluorescence microscopy (SRM) techniques. As a joint effort by researchers in multiple disciplines, including chemistry, computer sciences, engineering, and optics, the development of SRM has its own place in the long history of light-optical microscopy, culminating in the 2014 Nobel Prize in Chemistry being awarded to Eric Betzig, Stefan Hell, and William E. Moerner for their achievements in the advancement of single-molecule detection and super-resolution imaging [2]. More precisely, these researchers succeeded in developing revolutionary new microscopy techniques that can be used, for example, in the investigation of fluorescent cell samples down to the level of individual molecules, that is, they cleared the way for new approaches that have proven invaluable for a wide range of applications in biomedical research. This is due to the fact that after specific labeling of a target structure with fluorescent markers, a fluorescence readout can be analyzed with respect to its spatial and temporal distribution, and thus it provides great detail about the underlying structure [3]. As the background in fluorescence imaging is typically close to zero, the resulting contrast allowed even the detection of single molecules [4]. Despite these developments, none of the novel SRM techniques has so far invalidated Abbe's (1873) or Rayleigh's (1896) limits for the resolution of light-optical microscopy; methods of circumventing these limitations have been discovered. By implementing these methods it became possible for the first time to, for example, directly observe the molecular machinery of life by far-field light microscopy.

This introduction presents the basic physical concepts behind the limits in optical resolution and offers an up-to-date diachronic overview of some important landmarks in the development of SRM methods. The next two chapters focus on the physicochemical background (Chapter 2) and required hardware and software (Chapter 3). The next four topic-specific chapters are dedicated to a description and evaluation of structured illumination microscopy (SIM) (Chap-

*Super-Resolution Microscopy*, 1. Edition. Udo J. Birk.

ter 4), localization microscopy, and in particular single-molecule localization microscopy (SMLM) (Chapter 5), stimulated emission depletion (STED) microscopy (Chapter 6), and multi-scale imaging with a focus on light-sheet fluorescence microscopy (LSFM) and optical projection tomography (OPT), as well as on sample preparation techniques such as clearing and expansion microscopy (ExM) (Chapter 7). These application-oriented chapters are not restricted to a mere description of the respective techniques but offer a thorough discussion and evaluation of the specific potentials and problems of the various methods. Each of these advanced light-optical microscopy techniques responds in its own specific way to the research question and challenges at hand, and each of them comes with its own set of benefits and disadvantages. The discussion (Chapter 8) finally tries to push the limits by shedding light on potentially promising progressive approaches and future challenges in this ever-growing and extremely fast developing field. A particular focus in all of the discussions will be on the application of advanced light-optical microscopy in studies of biological cell samples.

In the visible range of the electromagnetic spectrum, cells can be considered thick, transparent objects that can be analyzed in three dimensions by means of far-field light microscopy either after fixation in a preserved state or possibly as live samples. However, the images produced by this analysis method lack structural information owing to the limited resolution of light microscopy. In recent years, a number of methods of fluorescence microscopy have been developed to narrow down the spread of the blur in microscopic images or to facilitate the separate detection (localization) of individual fluorescent molecules within samples and, thus, to prevent the "Abbe limit of microscopic resolution" from being applicable to the final microscopic image, resulting in the transition from microscopy to nanoscopy. The realization of focused nanoscopy-based STED and localization microscopy-based photoactivated localization microscopy (PALM) techniques represents culminating points of a long history of attempts to overcome the so-called Abbe limit: In 1873, Ernst Abbe, the colleague of Carl Zeiss, in his pioneering developments of advanced microscopy, stated that "[…] the limit of discrimination will never pass significantly beyond half the wavelength of blue light […]," which corresponds to approximately 200 nm. A similar limit for the possibility to distinguish two "point-like" luminous objects was given by Lord Rayleigh in 1896. Point-like means that the dimensions are much smaller than the wavelength used for imaging. From this time on, for about a century, the 200 nm value of the Abbe limit has generally been regarded as the absolute limit for obtaining structural information by far-field light microscopy. However, already in his famous contribution (1873) on the fundamental limits of optical resolution achievable in (far-field) light microscopy, Abbe stated that the resolution limit of about half the wavelength used for imaging is valid only "[…] so lange nicht Momente geltend gemacht werden, die ganz außerhalb der Tragweite der aufgestellten Theorie liegen […]."[1)] As seemingly foreseen by Abbe, only by deviating from

1) Which translates as "[…] as long as no different conditions are introduced that are completely beyond the theory stated here […]" [UB].

the experimental conditions stated in his original work could super-resolution by STED and PALM be achieved.

## 1.1 Classical Resolution Limit

In 1873, Ernst Abbe derived from theoretical considerations a criterion for the resolution limit of a light microscope. The considerations that led to its formulation are as brilliant as they are simple: He understood that an object consisting of small structural features gives rise to diffraction, which is known to be stronger for smaller structures. The plethora of structural features present in a real object might be approximated locally by a superposition of stripes of different orientations, stripe widths, and strengths. This will help us in what follows to understand the concepts behind the image blur. Let us consider a fine grating structure with lattice constant $d$ (spacing between two stripes), embedded in a medium with refractive index $n$, which is *illuminated centrally* with light of wavelength $\lambda/n$ ($\lambda$ being the vacuum wavelength). This will result in constructive interference of order $m$ observed under an angle $\alpha$ if the following condition is fulfilled:

$$\frac{m\,\lambda}{n} = d\,\sin(\alpha)\,. \tag{1.1}$$

When imaged by a lens, such an interference pattern will only be transmitted under the condition that, in addition to the central non-diffracted beam, at least the $m = \pm 1$ orders are collected by the lens, i.e., two fine object features have a minimum distance $d_{\text{centr.illum.}} = \lambda/(n\sin(\alpha))$. If oblique illumination is used, the minimum distance $d$ for which diffraction arising from the structure is collected by the lens is half the value of $d_{\text{centr.illum.}}$. From this Abbe derived his famous formula for the resolution limit in optical microscopy [5]:

$$d = \frac{\lambda}{2\,n\sin(\alpha)}\,, \tag{1.2}$$

which describes the minimum distance $d$ of two structural features to be resolved by the microscope, where $n\sin(\alpha)$ is the numerical aperture of the detection objective lens, $n$ is the refractive index of the sample, and $\alpha$ is half of the opening angle defined by the rays of light that are detected by the objective lens (acceptance cone); $\alpha$ is the so-called half-aperture angle of the objective lens.

In general terms, Abbe stated a formula for the smallest distance $d$ that two point-like object details can have so that they can still be discriminated (resolved) by microscopy. According to his formula (1.2), the smallest distance $d$ is determined by the vacuum wavelength $\lambda$ of the light used for imaging and the numerical aperture $n\sin(\alpha)$. For a perfect lens with no spherical aberration, the intensity of the *2D diffraction pattern* of such a single "point source" in the (perfect) focal plane is shown in Figure 1.1a. This diffraction pattern is described [6]

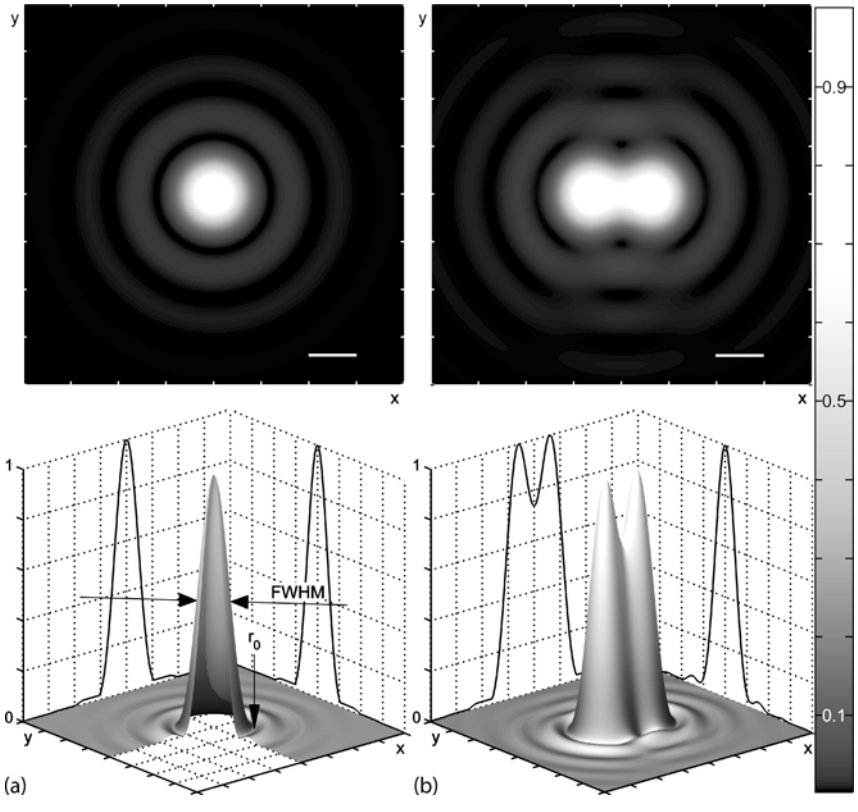


**Figure 1.1** Microscopic image of a "point source" (a) or two "point sources" in close proximity (b). Scale bar equals full width at half-maximum (FWHM) of the diffraction pattern of a single "point source." See text for numeric values.

by the formula

$$I(v) = I_0 \left( \frac{2J_1(v)}{v} \right)^2 , \tag{1.3}$$

where $J_1$ is the first-order Bessel function of the first kind, and $v$ is the (generalized) lateral optical coordinate, related to the image coordinate $r = \sqrt{x^2 + y^2}$ by

$$v(r) = r\frac{2\pi}{\lambda} n \sin(\alpha) = r\frac{2\pi}{\lambda} \mathrm{NA} . \tag{1.4}$$

Knowing the lateral magnification of the microscope system, the image coordinate $r$ can easily be transferred to the object coordinate space, i.e., the coordinates within the sample.

The diffraction pattern in the axial direction is responsible for having point-like objects imaged as elongated structures. The distribution of the diffraction pattern

in the axial direction differs from that in the lateral direction (Equation 1.3). It can be derived [7] (in good approximation) as

$$I_{\text{axial}}(u) = I_0 \,\text{sinc}\left(\frac{u}{4}\right)^2 , \tag{1.5}$$

where $\text{sinc}(z) := \sin(z)/z$, and $u$ is the generalized axial optical coordinate, which depends on the $z$-displacement $\delta = z' - f$, i.e., on the distance to the ideal (paraxial) focal plane, as follows:

$$\begin{aligned} u &= \frac{2\pi}{\lambda}\frac{\text{NA}^2}{n}(z' - f) \\ &= \frac{2\pi}{\lambda}\frac{\text{NA}^2}{n}\delta . \end{aligned} \tag{1.6}$$

In 1896, Lord Rayleigh put forward his formula for the resolution of an optical instrument, in particular of a light microscope [8], yielding values for the resolution very similar to those obtained by Ernst Abbe. His starting point was the analytical solution of the diffraction pattern of two such "point sources" (Figure 1.1b). By his reasoning, the two sources may be "resolved" if the second source is located at a distance equal to or larger than $r_0$, the first minimum of the diffraction pattern of the first source. The position of the first minimum $r_0$ of Equation 1.3 is given by the first root of the Bessel function $J_1(v)$: As a numerical approximation we obtain $v(r_0) = 3.83$, or $r_0 = 0.61\lambda/\text{NA}$. The central maximum up to the radius $r_0$ is called an *Airy disk* of the diffraction pattern. For two objects to be resolved according to the Rayleigh criterion, they must have a minimum distance of

$$d_{\text{min}} = r_0 = 0.61\frac{\lambda}{n\sin(\alpha)} = 0.61\frac{\lambda}{\text{NA}} . \tag{1.7}$$

In the simulations shown in Figure 1.1, however, the signals are placed 1 FWHM apart of the diffraction pattern of a single "point source." The relation between FWHM and $d_{\text{min}}$ is as follows [6]:

$$\text{FWHM} = \frac{0.51}{1.22}\text{AU} , \tag{1.8}$$

where AU is the typical unit used in microscopy called an Airy unit (1 AU = 2 $r_0$), indicating the diameter of the Airy disk. For practical reasons, instead of using $d_{\text{min}}$, which is difficult to measure in noisy data, often the FWHM is used as a resolution criterion, though it is somewhat smaller in value than the resolution limit stated by Lord Rayleigh. As can be seen from Figure 1.1, two objects placed at a distance of 1 FWHM can still be resolved in the absence of noise. Of course, both equations for the resolution (Equations 1.2 and 1.7) are idealized because they do not take, for example, pixelation into account (see also Section 3.2.1 on the localization of emitters).

The derivation of the optical resolution according to Abbe makes use of scattering as a contrast within the sample. Scattering occurs for both coherent and incoherent illumination. Resolution in the transmission microscope, however, is

different for coherent and for incoherent illumination [7]. In the case of fluorescence, the light emitted by different fluorophores is generally considered to be incoherent because of the typical fluorescence lifetimes, which are in the nanosecond range.

The intensity distribution described by Equation 1.3 is normalized to a peak intensity of 1. If instead it is normalized such that the area under the curve is equal to 1, it describes the probability of detecting a photon emitted by the "point source" at $\nu$ $\mathrm{d}\nu$, and similarly for the axial direction. For this reason, the distributions given by Equations 1.3 and 1.5 (using appropriate normalization) are also called the *point spread function* (PSF) in optical imaging. In signal processing, this corresponds to the impulse response function.

In many practical applications, for example in localization microscopy, it is of interest to measure the peak position of this diffraction pattern, which in the absence of noise and with infinitesimal sampling would be given by the spread of this distribution, as calculated by

$$\sigma_{\mathrm{PSF}} = \int_{-\infty}^{\infty} \nu^2 I(\nu)\ \mathrm{d}\nu\ . \tag{1.9}$$

Paraxial approximation was used in the derivation of Equation 1.3. Nevertheless, the integral $\int_{-\infty}^{\infty} I(\nu)\ \mathrm{d}\nu$ is finite. However, using the same derivation and approximations, Equation 1.9 does not converge. A practical way to deal with this – which in fact is used in most applications – is to restrict the evaluation to the central maximum. This is well justified: The central maximum (Airy disk) contributes by approximately 84% to the overall focal-plane intensity, independently of the numerical values for wavelength and NA. Consequently, for most practical implementations, instead of the analytical expression of the intensity distribution inside the Airy disk (Equation 1.3), a Gaussian approximation is used. This substitution using a Gaussian probability distribution has an effect on the accuracy when determining the peak position, which will be discussed in Section 3.2. More recently, especially in three-dimensional (3D) applications, cubic splines have been employed to better approximate the shape of the experimental PSF [9].

Using the PSF to describe the effect of diffraction on a "point source," the imaging process can be represented by

$$g(\vec{r}) = \int_{-\infty}^{\infty} f(\vec{r'})\,\mathrm{PSF}(\vec{r}, \vec{r'})\ \mathrm{d}\vec{r'}\ , \tag{1.10}$$

where $\vec{r}$, $\vec{r'}$ are 3D position coordinates, $g$ is the image, $f$ is the object. If the PSF is the same for every position in the sample and depends linearly on the light intensity emanating from the sample, then each part of the object is blurred by the same PSF [10]. In this case, the second part of the integrand (i.e., the PSF) depends only on the relative coordinate $(\vec{r} - \vec{r'})$, and the system is called linear shift invariant (LSI). Equation 1.10 is then simply a convolution. The imaging process can

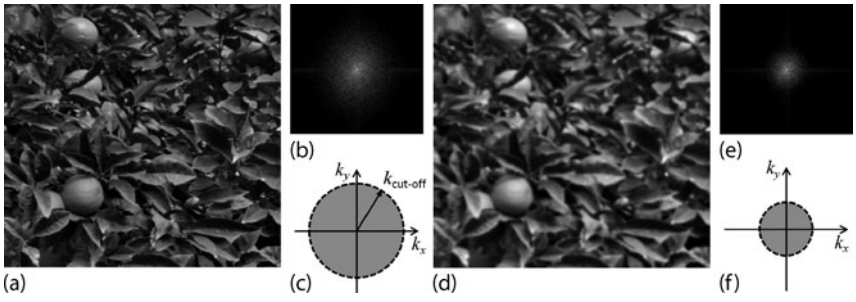


**Figure 1.2** Details from two photographs of a mandarin orange tree. The left part depicts the high-resolution data (a) and its Fourier transform (b). In the representation of the Fourier transform, a decomposition of image (a) in terms of "spatial frequencies" is done. Average intensity and slowly varying image features are represented in the center, while fine details (small structures) are located toward the periphery. A schematic of the frequencies present in the image is illustrated in (c). The right part shows the same data recorded with lower resolution, i.e., with increased blur (d), together with its Fourier transform (e). The reduction of fine structural details (i.e., lack of high-frequency content) is apparent from the schematic outline of the spatial frequencies present (f).

now be described using the Fourier transforms $G$ and $F$ of $g$ and $f$, respectively:

$$G(\vec{k}) = F(\vec{k})\,\mathrm{OTF}(\vec{k})\,. \tag{1.11}$$

In this equation, OTF is the Fourier transform of the intensity PSF, the so-called *optical transfer function* (OTF), and $k$ is the spatial wave vector (or spatial frequency). Because of diffraction, fine structural details are not transmitted in a microscope. Thus, the PSF is band-limited, which means that the OTF is zero for high frequencies beyond a cut-off frequency $k_{\text{cut-off}}$. This is schematically illustrated in Figure 1.2: Two versions of a photograph are shown (a) and (d) together with the respective strength of the Fourier transforms (b) and (e). The concept of the spatial frequencies present in the image are depicted in (c) and (f) respectively. The crisper image data (a) can be associated with a broad range of spatial frequencies present, indicative of a "broad" OTF of the imaging system. In contrast, an image taken at low resolution (b) has a much narrower OTF. The regions in which the OTF is non-zero (or above the noise level) is referred to as the "support" of the OTF. The cut-off frequency can also be used as a measure for the resolution of the microscope system. In analogy to the considerations by Ernst Abbe, the cut-off frequency of an optical microscope is given by $k_{\text{cut-off}} = \pi\mathrm{NA}/\lambda$.

### 1.1.1
### Examples of Microscopic Imaging without Using Visible Light

Ernst Abbe developed his famous formula by considering scattering arising from a sample itself in a manner similar to a Fourier decomposition of the sample structure [11]. For the sample structure to be imaged, the minimum requirement is that the $\pm 1$ order of the scattered signal must be detected by the objective lens.

The same formula can be derived from general considerations on diffraction in the context of matter waves, in which case the wavelength used for imaging, i.e., the wavelength for the detection of the contrast, is given by the de Broglie wavelength [12]. Equation 1.2 can be used, for example, to calculate the resolution in electron microscopy (EM) [13]. For an acceleration voltage of 75 keV, a de Broglie wavelength of approximately 0.22 nm was originally calculated [14], indicating that the resolution is orders of magnitude better than for optical imaging, and much more detail may be observed in electromicrographs. An additional relativistic correction must be made to account for the electron velocity approaching the speed of light, $c$:

$$\lambda_{e^-} \approx \frac{h}{\sqrt{2m_0E\left(1+\frac{E}{2m_0c^2}\right)}}, \tag{1.12}$$

with $h$ being Planck's quantum, $m_0$ the rest mass of the electron, and $E$ the acceleration voltage applied.

In addition to these diffraction-based imaging approaches in transmission electron microscopy (TEM) [14], other microscopy techniques that do not rely on visible light either have been established. These include, for example, scanning tunneling microscopy (STM) [15] and atomic force microscopy (AFM) [16]. All of these non-optical techniques place a number of restrictions on samples. Some of the more severe disadvantages, for instance, in using electron microscopy (EM) are that experiments are generally performed with the samples placed in a vacuum, which requires a special sample preparation, and often coating with a metal film is also necessary. Nonetheless, these techniques played a major role in the discovery of essential elements of chromatin nanostructure, such as the nucleosomes [17, 18] and other important features (for review see [19]).

All microscopy techniques that avoid the use of visible light have in common that it is not easy to label and distinguish multiple types of targets inside cells, so it is difficult to achieve specific contrast. Typically, immunostaining using gold nanoparticles can be done for EM; however, before the advent of electron spectroscopic imaging (ESI), there was no easy way to perform energy-discriminating imaging (i.e., to use different wavelengths in the same acquisition sequence), and so the number of different spectral signatures was severely limited. Modern TEM allows energy filters to be used, which produces a contrast for specific chemical elements. In biological tissue, a number of different chemical elements can be used for discriminating imaging. However, each of these elements of which biological tissue is composed is typically found simultaneously in a plethora of proteins, lipids, amino acids, and others alike and is thus not specific. Early approaches of electron spectroscopic imaging of the nucleus made use of phosphorus and nitrogen mapping, providing sufficient contrast and resolution to distinguish protein-based from nucleic acid-based supramolecular structures [20]. Last but not least, the irradiation of a sample with accelerated electrons gives rise to ionization, which in turn correlates with structural changes within the sample such as atomic displacements, migration, and desorption effects [21].

For the aforementioned reasons, and in comparison to EM, fluorescence microscopy has a couple of advantages: (1) multiple specific cellular components may be observed from within the same sample through molecule-specific labeling and (2) the requirements for sample preparation and observation are modest. Although it is not necessarily true for all advanced super-resolution light microscopy realizations, in principle light microscopy allows the observation of structures inside a live sample in real time. As a consequence, light microscopic techniques play a vital role in the life sciences.

### 1.1.2
### Early Concepts of Enhanced Optical Resolution

Once the theoretical resolution of microscopic detection was understood, work related to the further optimization of microscopic illumination started. Shortly after Abbe, realizing that the final microscopic image resolution also depended on the coherence of the illumination light, August Köhler achieved precise control over the illumination. Despite this, it took some time to realize that the effect of illumination can, in principle, be used to even enhance the resolution beyond the theoretical limit given by diffraction in microscopic detection. On November 7, 1957, Marvin Minsky filed a US patent application on the construction of a *confocal microscope* [22]. The basic idea was to focus a strong light source point by point onto a sample, thereby scanning an object with a focused beam and to register the transmitted/reflected light also point by point. For enhanced resolution, a pinhole in front of the light detector rejects light originating from sample parts above and below the focal plane. At the time, however, the laser was yet to be invented, and Minsky's concept for a transmitted/reflected light confocal microscope, called a "microscope apparatus," remained largely unnoticed until the 1980s. Only upon equipping the instrument with suitable laser light sources did the then termed "confocal laser scanning microscope (CLSM)" become a valid alternative to conventional microscopy [23, 24], with its tremendous success especially in the fluorescence mode.

The basic principle of CLSM is illustrated in Figure 1.3. The "point source" obtained from a laser light source may be focused with high efficiency as a diffraction-limited spot into the focal plane of the objective lens. This small spot may be scanned within the focal plane, for example by a set of mirrors, and at each scan position the fluorophores subjected to illumination by this focal spot emit fluorescence, which is collected by the objective and directed to the detector. Typically a single-element detector, such as a photomultiplier tube (PMT) or a highly sensitive photodiode, is used, requiring descanning of the detected light in order to be able to direct the fluorescence signal collected by the objective lens towards the point detector. This is achieved by having the scanning device (e.g., the scan mirrors) not only in the illumination but also in the detection path. By moving the scanning mirror (or alternatively by moving the sample), the position of the focused diffraction-limited illumination spot is changed and the fluorescence signal from neighboring "pixels" is recorded.

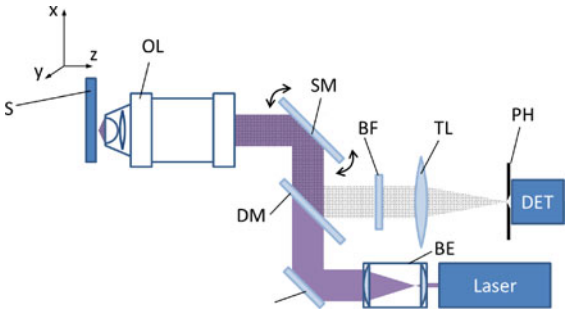


**Figure 1.3** Schematic representation of a confocal laser scanning microscopy (CLSM) setup. Laser light sources for fluorescence excitation are collimated and expanded using a beam expander (BE) of fixed or variable output beam width. The beam is subjected to a scanning mirror (SM) device, typically with two rotating mirrors for deflecting the beam in the *x*- and *y*-directions. The excitation beam illuminates the back focal plane of an objective lens (OL), resulting in a diffraction-limited illumination spot within the focal plane of the OL, i.e., within the sample. Fluorescence light is collected via the same OL and descanned on the SMs before it is separated from the excitation light by a dichroic mirror (DM). Residual laser light is suppressed by a blocking filter (BF). A tube lens (TL) focuses the fluorescence light onto a pinhole (PH) to prevent out-of-focus light from entering the detector array (DET). An equivalent setup without an excitation PH was proposed by Cremer and Cremer in 1978 [23].

The light intensity of the illumination (excitation) focal spot is distributed according to the illumination PSF. If – in an ideal situation – the back focal plane of the objective lens is fully illuminated with equal intensity, corresponding to a circular aperture, the PSF displays a pattern according to Equation 1.3 with a central "Airy disk" (Figure 1.1) having a radius proportional to $\lambda/\mathrm{NA}$. The overall probability of detecting a fluorescent molecule that is in the focal plane but positioned off-axis, i.e., not centered in the PSF, is given by the product of the probability of exciting it times the probability of detecting it. While the former is given by the illumination $\mathrm{PSF}_{\mathrm{ill}}$, the latter is given by the detection $\mathrm{PSF}_{\mathrm{det}}$, and the total $\mathrm{PSF}_{\mathrm{tot}}$ is given by

$$\mathrm{PSF}_{\mathrm{tot}} = \mathrm{PSF}_{\mathrm{ill}} \times \mathrm{PSF}_{\mathrm{det}} \,. \tag{1.13}$$

As with conventional wide-field microscopy, the resolution of a CLSM is determined by the width of the PSF. Additionally, the scanning (displacement of the focal spot) needs to match the width of the PSF: The smaller the focal spot is, the more meaningful pixels can be acquired in the image, and each pixel will contain information from a smaller region in the sample. As a consequence, the image will be less blurred. While the confocal microscope is mostly used for its ability to suppress out-of-focus light [25], theoretical considerations show that the optical resolution can be enhanced by a factor of 1.4 in the object plane [25–27], and a true optical resolution of about one wavelength along the optical axis (i.e., perpendicular to the object plane) can be obtained [28]. For a detailed historical review please see, for example, [29].